Available online at www.sciencedirect.com

ScienceDirect

journal homepage: www.elsevier.com/locate/he

Interaction between $Li_2Mg(NH)_2$ and CO: Effect on the hydrogen storage behavior of the $Li_4(NH_2)_3BH_4$ doped $Mg(NH_2)_2$-2LiH composite

N.S. Gamba [a,*], G. Amica [a,b], P. Arneodo Larochette [a,b], F.C. Gennari [a,b]

[a] Consejo Nacional de Investigaciones Científicas y Técnicas (CONICET) and Centro Atómico Bariloche (CNEA), Av. Bustillo 9500, R8402AGP, S.C. de Bariloche, Río Negro, Argentina

[b] Instituto Balseiro, Universidad Nacional de Cuyo, Argentina

ARTICLE INFO

Article history:
Received 30 September 2016
Received in revised form
16 November 2016
Accepted 18 November 2016
Available online 9 December 2016

Keywords:
Hydrogen purification
Hydrides
Amides
Carbon monoxide
Cyanamide

ABSTRACT

Metal hydrides have been studied as a promising solution for the hydrogen recovery from gas mixtures of industrial processes. However, scarce information is available about the behavior of amides as hydrogen purification material. In this work, the tolerance against CO, hydrogen sorption kinetics and the thermodynamics of the $Li_4(NH_2)_3BH_4$ doped $Mg(NH_2)_2$-2LiH composite after repetitive dehydrogenation and rehydrogenation cycles with 0.1 mol% of CO-H_2 mixture were investigated. A progressive degradation of the hydrogen storage capacity of the material and an improvement in the dehydrogenation rate (50%) was observed for the composite after 20 cycles of the CO containing gas mixture. The formation of Li_2CN_2 and MgO, which are the main responsible for the deterioration of the hydrogen storage properties, was confirmed by Fourier transform infrared spectroscopy (FTIR) and X-ray powder diffraction (XRPD). For the first time, the reaction between pure CO and the dehydrogenated product $Li_2Mg(NH)_2$ was demonstrated. This reaction is fast and produces mainly Li_2CN_2 and MgO as solid products. When a high CO pressure was diluted with H_2 (mol ratio 1:8), the reactivity of $Li_2Mg(NH)_2$ with CO was notably reduced and mainly MgO formation was detected. No clear reaction of CO with $Mg(NH_2)_2$ was detected by FTIR, XRPD and volumetric measurements. Evaluation of the reactivity of CO with $LiNH_2$-LiH, $Mg(NH_2)_2$-2LiH and $LiBH_4$ systems provides the following decreasing ranking of reactivity: $[NH]^{2-} > [NH_2]^- > [BH_4]^-$.

Introduction

Different processes are used to produce hydrogen, such as steam reforming from hydrocarbons, partial oxidation of methane and coal gasification among others. Unfortunately, the hydrogen obtained is usually accompanied by other gases, such as O_2, H_2O, H_2S, CO_2 and CO. Thus, an intermediate step is generally required for its separation and purification in order to obtain high purity hydrogen, both for its storage as well as for its usage in different applications. Within the available options, metal hydrides can be used for hydrogen

* *Corresponding author*. Fax: +54 294 4445190.
E-mail address: gamba.nadia@gmail.com (N.S. Gamba).
http://dx.doi.org/10.1016/j.ijhydene.2016.11.136

purification due to its capacity to absorb selectively hydrogen from a gas mixture [1,2]. Various studies have been carried out using these materials to purify hydrogen mainly from gas mixtures containing CO impurities. As a general behaviour, it was found that hydride forming alloys severely decrease their hydrogen storage capacity with increasing CO concentration [3–6]. The studies involving hydrogen purification and storage by metal hydrides are mostly related to AB_5-type materials such as $LaNi_5$ or modified $LaNi_5$ by partial substitution (Sn, Co, Mn, Al) [2,6–9]. Han et al. investigated the cyclic stability of the $LaNi_5$ alloy with hydrogen containing CO as impurity. They found that the CO molecule can be easily adsorbed on the alloy surface, producing poisoning and depressing its hydrogen storage capacity [6]. To avoid or reduce poisoning by CO, several methods have been proposed which involve changes in the alloy composition and/or surface modifications, such as the plating method, the fluorination treatment and oxidation-reduction method [2,7]. Lototsky has shown that AB_5-typo materials modified by surface treatment are feasible candidates for hydrogen separation from a gas containing a CO_2 and CO mixture [7,8]. More recently, the $LaNi_{4.73}Sn_{0.27}$ alloy has shown a deterioration in the kinetics with cycling in presence of CO (10 and 100 ppm), without loss of hydrogen storage capacity [9]. However, the CO separation ability of the AB_5 is dependent of the temperature and CO concentration in the gas mixture.

On the other hand, there are few studies on hydrogen purification using MgH_2-based materials. Dehouche et al. showed the effect of CO impurity (110 ppm) on hydrogen storage properties after cycling of the MgH_2-V composite. Furthermore, the effect of other impurities such as N_2, O_2 and CO_2 in the same composite was evaluated [3]. The presence of CO as impurity deteriorates the advantageous hydrogen dissociative chemisorption properties of vanadium. The kinetics deterioration and the capacity loss of the composite due to the MgO_x formation was demonstrated [2].

Moreover, studies of the hydrogen sorption properties of amides as well as their tolerance to cycling using hydrogen-rich gas mixtures with impurities are limited. The CO_2-H_2 mixture, consisting of 20% CO_2 and 80% H_2 as a product of the steam reforming of natural gas, was used for hydrogen storage in Li_3N [10,11] and $LiNH_2$-Li_3N [12]. These authors observed that the hydrogen storage properties of the Li-N-H system were unaltered by the presence of CO_2. Recently, Sun et al. investigated a series of contaminants such as N_2, CH_4, O_2 [13] and CO [14,15] using $2LiNH_2$-MgH_2 as storage system. These authors reported that the hydrogen desorption properties and the phase structure were unaffected by N_2 and CH_4 impurities. However, when a mixture of O_2 (0.1 mol %)-H_2 was employed, $LiNH_2$ and MgO were identified on the surface of the material with the consequent irreversible loss in the hydrogen storage capacity. Additionally, the negative effect of CO (1 mol %) impurity on the hydrogen storage properties of $2LiNH_2$-MgH_2 was shown. In fact, a reduction in the dehydrogenation rate and a loss in the storage capacity were noted after 6 cycles. This is mainly due to the formation of Li_2CN_2 and MgO phases. The authors propose a possible reaction, but no additional investigations to prove this statement were performed.

The Li–Mg–N–H system is considered as a promising material for hydrogen storage. The hydrogen desorption reaction of the $Mg(NH_2)_2$–2LiH composite occurs in two-steps, reactions (1) and (2), with the $Li_2Mg_2(NH)_3$ phase as intermediate. The complete dehydrogenation process leads to the $Li_2Mg(NH)_2$ phase, according to reaction (3).

$$2Mg(NH_2)_2 + 3LiH \rightarrow Li_2Mg_2(NH)_3 + LiNH_2 + 3H_2 \quad (1)$$

$$Li_2Mg_2(NH)_3 + LiNH_2 + LiH \rightarrow 2Li_2Mg(NH)_2 + H_2 \quad (2)$$

$$\text{Complete Reaction: } Mg(NH_2)_2 + 2LiH \leftrightarrow Li_2Mg(NH)_2 + 2H_2 \quad (3)$$

However, this system has some kinetic constraints and for this reason catalysts are required to increase the sorption rates and obtain lower desorption temperatures. Several studies were done using different additives to improve the hydrogen storage properties of the $Mg(NH_2)_2$-2LiH system. Catalysts, such as metal hydrides (CsH, CaH_2, RbH, KH) [16,17], borohydrides ($LiBH_4$, $Li_4BN_3H_{10}$, $Ca(BH_4)_2$, $Mg(BH_4)_2$) [18–21], halides ($CaBr_2$, LiBr, LiI, RbF, KF $TiCl_3$, VCl_3) [22] and other compounds were employed. These catalysts reduced the activation energy barrier and improved the thermodynamics properties of the system.

In particular, we selected the $Li_4(NH_2)_3BH_4$ as dopant of the Li-Mg-N-H system because the presence of $Li_4(NH_2)_3BH_4$ improves the hydrogen sorption properties as was evaluated in a previous work of the group [19]. The $Li_4(NH_2)_3BH_4$ doped sample increases the dehydrogenation and hydrogenation rates twice and twenty times, respectively, at 200 °C. The function of $Li_4(NH_2)_3BH_4$ was catalytic, decreasing the activation energy of hydrogen desorption with respect to the undoped sample.

The role of the additive in the reaction mechanism of the system was shown according to the following reaction [19]:

$$1/3Li_4(NH_2)_3BH_4 + Li_2Mg_2(NH)_3 + LiH \rightarrow 2Li_2Mg(NH)_2 + 1/3LiBH_4 + H_2 \quad (4)$$

Then, the $LiBH_4$ obtained by reaction (4) reacts with $LiNH_2$ produced by reaction (1) to form $Li_4(NH_2)_3BH_4$ again:

$$1/3LiBH_4 + LiNH_2 \rightarrow 1/3\ Li_4(NH_2)_3BH_4 \quad (5)$$

Considering the participation of $Li_4(NH_2)_3BH_4$ in the dehydrogenation mechanism the difference observed in the PCI curve at 200 °C for LM and LMB sample was explained [19].

In view of the fast sorption kinetics of the $Li_4(NH_2)_3BH_4$ doped $Mg(NH_2)_2$-2LiH composite, this material was selected to further studies. The aim of the present work is to analyze the effect of CO as impurity on the dehydrogenation kinetics and hydrogen storage capacity, as well as studying the cycle durability of the $Li_4(NH_2)_3BH_4$ doped $Mg(NH_2)_2$-2LiH composite with CO (0.1 mol %) -containing H_2. Furthermore, the possible interaction mechanisms of the CO molecule with the composite with and without $Li_4(NH_2)_3BH_4$, during CO (0.1 mol%)-H_2 cycling, are discussed.

Experimental

Synthesis of the Li–Mg composite

$LiNH_2$ (95%), MgH_2 (98%), and $LiBH_4$ (90%) were purchased from Aldrich. All samples were handled in an MBraun Unilab argon-filled box, with oxygen and moisture levels lower than 5 ppm. For all studies, high purity hydrogen (Linde, 99.999%) and argon (Linde, 99.999%) were used. The sample preparation was carried out by mechanical milling of $2LiNH_2$-$MgH_2$and $2LiNH_2$-MgH_2-$0.2LiBH_4$, using a sequence of 15 min milling and 10 min pause in a planetary ball mill (Fritsch Pulverisette 6) under 0.1 MPa of argon. The samples were indicated as LM and LMB composites. They consist of $Mg(NH_2)_2$-2LiH and $Mg(NH_2)_2$-2LiH-$0.2Li_4(NH_2)_3BH_4$, respectively [19]. The milling conditions were 500 rpm with a ball to powder mass ratio of 53:1 for 20 h. To avoid NH_3 emission, the mill chamber was opened and manually mixed after 1 h, 3 h, 5 h, 10 h and 15 h to eliminate possible dead zones.

Characterization of the composites

Structural information of the as-milled and as-cycled samples was obtained by X-ray powder diffraction (XRPD, PANalytical Empyrean, Cu Kα radiation, graphite monochromator) and Fourier transform infrared spectroscopy analyses (FTIR, Perkin Elmer Spectrum 400 with MCT detector). During the XRPD data collection, the samples were maintained under Ar atmosphere using a tightly sealed holder to prevent their reaction with air. For IR spectroscopy measurements, the samples were grounded with dry KBr under purified argon atmosphere, pressed to pellets and placed in a specially designed airtight cell. Handling was done inside the glove box to avoid contact with air. Solid state IR spectra were obtained in the range of 4000–800 cm^{-1} with a resolution of 4 cm^{-1}. FTIR-gas analyses were performed on gases released after heating of LMB previously hydrogenated with CO (0.1 mol%)/H_2 mixture.

Hydrogen sorption kinetics and Pressure-composition isotherms (PCI) were obtained using modified Sieverts-type equipment, coupled with a mass flow controller. The sample was transferred in the glove box inside a stainless reactor which was connected to the Sieverts device. For kinetic measurements, gases with different compositions were considered. First, cycling was performed using pure H_2 and then the same experimental procedure was repeated using a mixture CO (0.1 mol%)-H_2. Before the first dehydrogenation, the sample was heated up to the reaction temperature (200 °C) under H_2 pressure of 6.0 MPa and kept at this temperature for 30 min. Dehydrogenation curves were obtained at 200 °C with gas back pressure of 0.05 MPa.The dehydrogenation rate values were obtained from the slope of the straight portion of the dehydrogenation curves, between 0.05 wt% and 1.5 wt%. The rehydrogenation curves were measured at 200 °C at a constant pressure of 6.0 MPa when H_2 or the CO-H_2 mixture were employed for cycling. In addition, pure CO was used to test the reactivity with $Mg_2(NH_2)_2$-2LiH and $Li_2Mg(NH)_2$ systems. PCI curves were measured at 200 °C. As regards PCI, a stationary state at 200 °C in each sample was required before measuring PCI at other temperatures [19]. The hydrogen contents reported in this paper are expressed as wt% considering the total mass of each mixture.

Results and discussion

Dehydrogenation behavior of the LMB composite during cycling under CO (0.1 mol%)-H_2

To analyze the tolerance to CO as impurity during hydrogen absorption/desorption cycling, the LMB sample was submitted to several cycles. The dehydrogenation curves obtained after hydrogen cycling with and without CO content at 200 °C are shown in Fig. 1. Although the first cycle looks similar independently of the gaseous atmosphere, the influence of CO is evidenced in the posterior cycles: the hydrogen storage capacity of the LMB composite seems to decrease and the hydrogen desorption rate increase. To clarify the comparison, Fig. 2 shows the evolution of the hydrogen storage capacity (Fig. 2A) and the dehydrogenation rate (Fig. 2B) with the cycle number after several consecutive cycles of sorption.

As a general characteristic, the composite hydrogen storage capacity decreases after successive sorption cycles. In terms of stability, a reduction of 22% of the initial capacity (4.9 wt%) was observed after 20 cycles of sorption with CO-H_2 mixture, in comparison with only 10% of deterioration for the cycling under pure H_2 (initial capacity 4.7 wt%). Regarding the dehydrogenation rate, the behavior is opposite with and without CO content: while dehydrogenation rate increases about 15% after 20 cycles when CO impurity is present, it decreases in more than 50% after 20 cycles with pure hydrogen. These results indicate that CO interacts with the hydrogen storage material limiting its storage capacity but favoring dehydrogenation rate. FTIR analysis of the gaseous dehydrogenation products does not provide evidence of the formation of NH_3 or other species. Only hydrogen was released, demonstrating that the Li–Mg–N–H system is able to separate hydrogen from CO-H_2 mixture but modifying the starting material. This behavior will be analyzed in the next section on the basis of the structural modifications experimented by the composite during CO-H_2 cycling.

PCI measurements were performed to evaluate the effect of cycling under CO-H_2 mixture. Fig. 3 shows dehydrogenation PCIs collected after the 10th and 20th cycles. As a reference, the PCI obtained after 10th cycle under pure hydrogen is also shown. It can be seen that all PCI curves exhibit a sloped plateau, being the pressure change in the plateau region higher for the material under pure hydrogen. Besides, the initial equilibrium pressure for the PCI curves of the LMB composite using CO-H_2 mixture is lower than the pressure measured with pure hydrogen, indicating that the improved dehydrogenation rate observed under CO-H_2 mixture is not related with a beneficial equilibrium hydrogen pressure. These differences suggest that different reactions are involved during dehydrogenation. In the case of the reference sample, the sloped plateau was associated to changes in the material constitution during dehydrogenation by a reaction that involves $Li_4(NH_2)_3BH_4$ and $Li_2Mg_2(NH)_3$ [19]. The presence of CO in the gaseous atmosphere seems to favor other reactions which decrease the initial equilibrium hydrogen pressure at

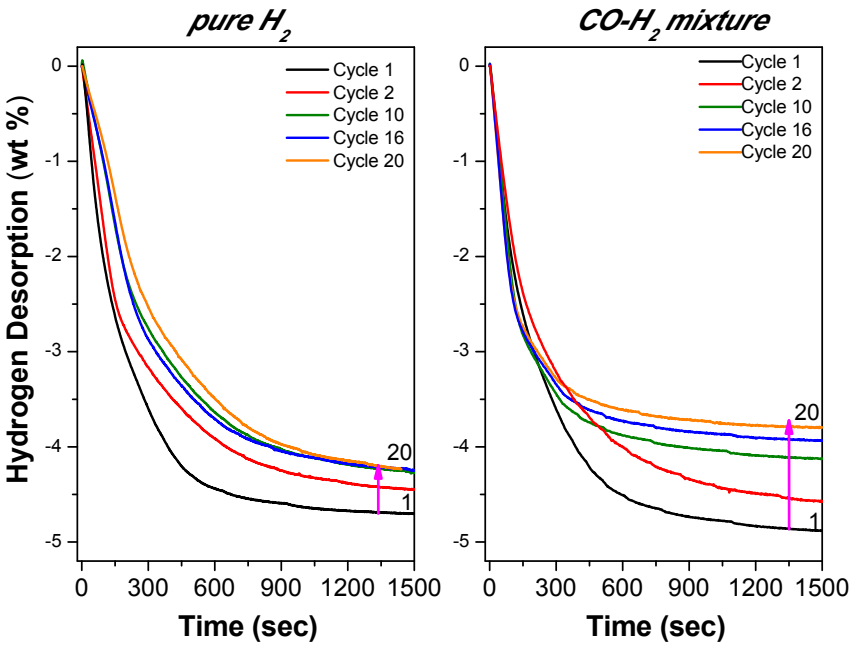

Fig. 1 – Dehydrogenation curves of the LMB composite at 200 °C after rehydrogenation at 6.0 MPa with H_2 and CO (0.1 mol%)-H_2 mixture.

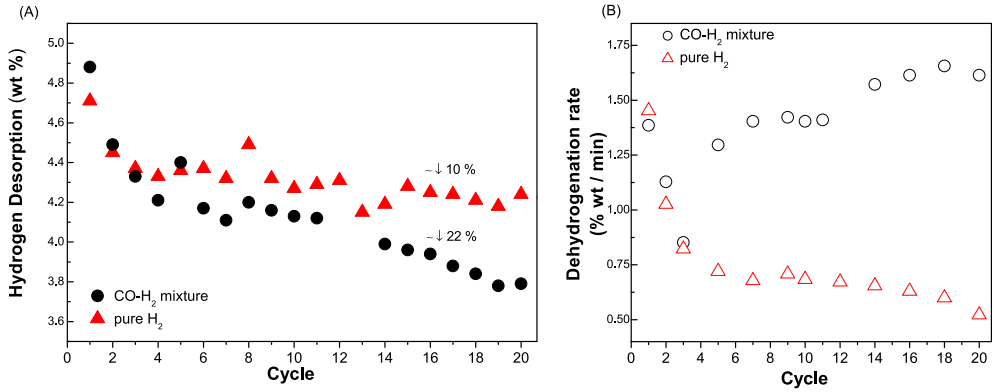

Fig. 2 – Evolution of: (A) the hydrogen storage capacity and (B) the dehydrogenation rate, with the cycle number for LMB composite at 200 °C. Absorption at 6.0 MPa pressure with pure H_2 or CO (0.1 mol%)-H_2 mixture; Desorption at 0.05 MPa pressure.

200 °C and deteriorate the thermodynamics properties of the composite.

Interaction between LMB composite and CO-H_2 gaseous mixture

In order to understand the interactions that occur after successive dehydrogenation and rehydrogenation cycles, the structural modifications of the LMB sample at different stages were studied by a combination of FTIR and XRPD. Figs. 4 and 5 show the FTIR spectra and XRPD patterns, respectively, obtained for the LMB sample after thermal treatment, dehydrogenation and rehydrogenation cycling based on ex-situ measurements. The FTIR spectrum of the LMB composite after milling displays broad peaks (Fig. 4a), from which $Mg(NH_2)_2$ is identified by its characteristic N-H vibrations at 3326 cm^{-1} and 3274 cm^{-1} simultaneously with $Li_4(NH_2)_3BH_4$ (3302 and 3244 cm^{-1}). The presence of residual $LiNH_2$ cannot be discarded (3313 cm^{-1} and 3258 cm^{-1}). The identification of a broad band at 2300 cm^{-1} by FTIR indicates the presence of B-H type bonds, associated with $Li_4(NH_2)_3BH_4$ compound. When the sample was submitted to thermal treatment under 6.0 MPa of CO-H_2 mixture at 200 °C (Fig. 4b), the FTIR bands became narrower and clearly allow the identification of $Mg(NH_2)_2$ and $Li_4(NH_2)_3BH_4$. No evidence about the presence of $LiNH_2$ was obtained. Then, the phases observed are the same as those detected after thermal treatment under pure H_2 [19].

The comparison of the FTIR spectra obtained after 10th rehydrogenation cycles using H_2 (Fig. 4c) or CO-H_2 mixture (Fig. 4d) show differences. In both cases, the vibrations of $Mg(NH_2)_2$ and $Li_4(NH_2)_3BH_4$ were identified as well as new bands of $Li_2Mg_2(NH)_3$ (3198 cm^{-1} and 3160 cm^{-1}) associated with incomplete rehydrogenation. However, a sharp band at 2149 cm^{-1} is only detected after cycling under CO-H_2 mixture.

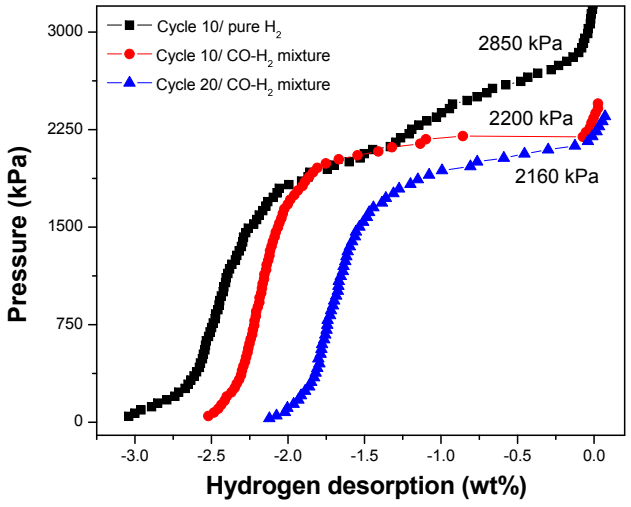

Fig. 3 – Dehydrogenation PCI curves of the LMB composite at 200 °C after the10th and the 20th rehydrogenation under 6.0 MPa CO-H_2 and 10th rehydrogenation under 6.0 MPa H_2.

This band could be related to the formation of Li_2CN_2, which was previously observed by Sun et al. [14]. The formation of lithium cyanamide is an evidence of the interaction between the LMB composite and CO. Moreover, the FTIR obtained after hydrogen desorption PCI of the cycled LMB sample (20th cycle under 6.0 MPa CO-H_2, Fig. 4e) shows additional evidence of the deterioration of the composite. The bands associated to the dehydrogenated state such as $Li_2Mg(NH)_2$ (3180 cm^{-1}) and $Li_2Mg_2(NH)_3$ were noted, simultaneously with that of Li_2CN_2 (2149 cm^{-1}). The vibrations referred to $Li_4(NH_2)_3BH_4$ were also detected, suggesting that the formation of Li_2CN_2 was more related to the interaction between CO and $Mg(NH_2)_2$/$Li_2Mg(NH)_2$ than with $Li_4(NH_2)_3BH_4$.

The XRPD patterns confirm the above interpretations (Fig. 5). From these patterns, the presence of $Mg(NH_2)_2$ and $Li_4(NH_2)_3BH_4$ as main phases were identified in the LMB composite after thermal treatment (Fig. 5a) and after cycling under pure hydrogen (10th cycle, Fig. 5b). No evidence about the formation of other compounds such as MgO or Li_2O was detected associated with prolonged cycling under hydrogen. In opposition, the XRPD pattern obtained after LMB rehydrogenation under CO-H_2 mixture (10th cycle, Fig. 5c) shows the most intense peaks of MgO. Further cycling with CO-H_2 mixture under equilibrium conditions (Fig. 5d) allows detecting the most intense peaks of Li_2CN_2 simultaneously with those of MgO in the desorbed state of the composite. Then, Li_2CN_2 and MgO formation was observed in the hydrogenated and dehydrogenated state. Therefore, the experimental evidence indicates that the formation of Li_2CN_2 and MgO was due to the irreversible reaction between LMB composite and CO. Although the reaction of CO with $Li_4(NH_2)_3BH_4$ cannot be discarded, $Li_4(NH_2)_3BH_4$ is identified even after prolonged cycling.

The structural modifications noted in the composite as a consequence of cycling with CO (0.1 mol%)-H_2 were the main responsible for its hydrogen storage properties. Different works using AB_5-type metal alloy reported a poisoning effect of CO that lead to complete loss of hydrogen storage capability [1,6]. In particular, Sun et al. informed an irreversible declination of both the hydrogen storage capacity of $Mg(NH_2)_2$-2LiH as well as the hydrogen desorption kinetic after six cycles under CO(1 mol%)-H_2 [14]. They related these results with the formation of Li_2CN_2 and MgO on the surface of the composite, which prevent the substance transmission during dehydrogenation process. In that work it was demonstrated that dehydrogenation rate can be recovered to the initial value

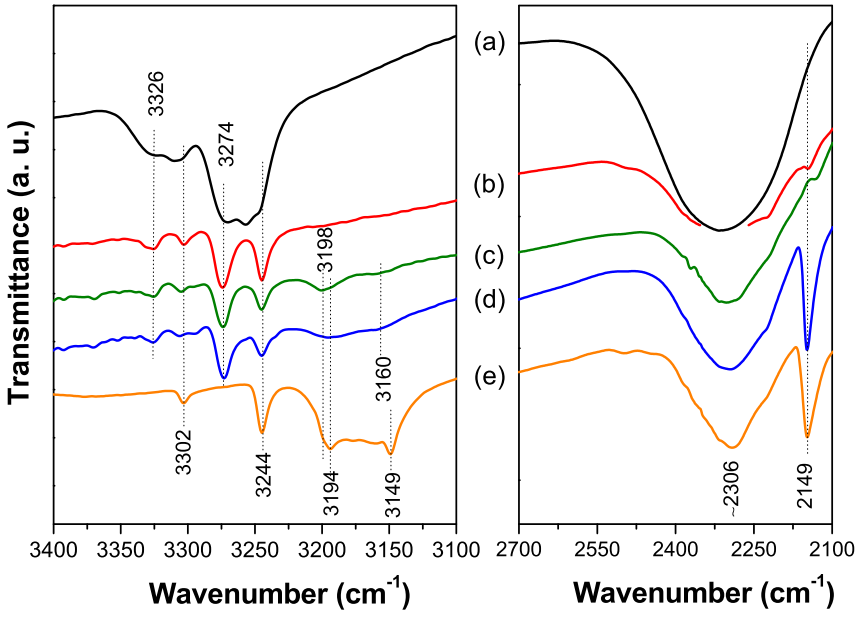

Fig. 4 – FTIR spectra of the LMB composite after: (a) milling, (b) treatment at 200 °C with 6.0 MPa CO-H_2, (c) 10th rehydrogenation under 6.0 MPa H_2, (d) 10th rehydrogenation under 6.0 MPa CO-H_2 and (e) dehydrogenation PCI of the sample after 20th rehydrogenation under 6.0 MPa CO-H_2.

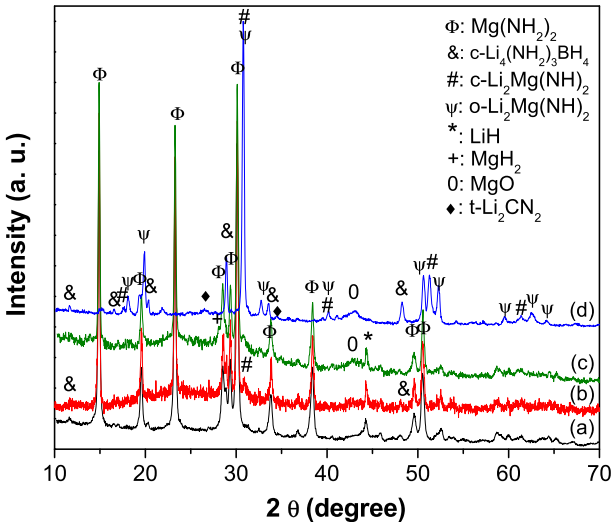

Fig. 5 – XRPD patterns of the LMB composite after: (a) treatment at 200 °C with 6.0 MPa H_2 (cycle 0), (b) 10th rehydrogenation under 6.0 MPa H_2, (c) 10th rehydrogenation under 6.0 MPa CO-H_2 and (d) dehydrogenation PCI of the sample after 20th rehydrogenation under 6.0 MPa CO-H_2.

after mechanical milling of the material. However, a permanent hydrogen storage capacity loss was observed. A similar tendency was found by these authors for the $Mg(NH_2)_2$-2LiH composite with KF as additive, because in addition to the formation of Li_2CN_2 and MgO, KF transformed to KCN [15]. In our case, the LMB composite (Figs. 1 and 2) displays a different behavior during CO-H_2 cycling using a low CO amount. On one hand, the hydrogen storage capacity decreases, which can be related with the irreversible formation of Li_2CN_2 and MgO. On the other hand, dehydrogenation rate increases, suggesting that Li_2CN_2 and MgO favor some rate controlling process. In fact, MgO could act as catalyst for the Li–Mg–N–H system [23] improving the dehydrogenation rate of the composite, as it was demonstrated previously. In addition, the high CO concentration used in the measurements of Sun et al. [14] favors the sintering of Li_2CN_2 and MgO on the surface, retarding further diffusion process. Then, both facts, the MgO formation and the lower CO content, are responsible for the enhancement of the dehydrogenation kinetics of the LMB composite. Considering that the equilibrium hydrogen pressure of the LMB decreases in the presence of CO but its dehydrogenation rate improves, other reactions than (1) and (2) are involved during dehydrogenation. The new pathway has a lower equilibrium hydrogen pressure than LMB but the same order than LM [19], with probably lower activation energy due to the presence of MgO.

Study of the interaction of pure CO with LMB and LM composites

To clarify if CO reacts with the dehydrogenated or hydrogenated composite and/or intermediate phases formed during hydrogen cycling, two different types of experiments were performed in a volumetric equipment.

First, the dehydrogenated state of LM and LMB composites as well as $LiNH_2$-LiH and $LiBH_4$ systems were contacted with pure CO (1.0 MPa) at 200 °C. The interaction was followed by measuring the amount of gas consumed (gas mol/sample mol) as a function of time (Fig. 6). For the dehydrogenated LM and LMB composites, it was observed that the reaction with CO displays a fast stage during 25 s, consuming between 0.55 and 0.60 gas mol/sample mol (Fig. 6a and b). After 50 s, the reaction seems to slowly reach the saturation at about 0.7 gas mol/sample mol. Clearly, CO reacts with the dehydrogenated state of $Li_2Mg(NH)_2$ independently of the presence of $Li_4(NH_2)_3BH_4$. On the other hand, pure CO displays a moderate or undetectable reactivity with $LiNH_2$-LiH and $LiBH_4$ systems, respectively (see Fig. 6c and d).

FTIR and XRPD analyses of the samples obtained after volumetric measurements (Fig. 6) allow to identify the phases formed by the interaction between CO and the composites (Figs. 7 and 8). For the LM and LMB composites, from the XRPD patterns it can be seen that the peaks of $Li_2Mg(NH)_2$ practically disappeared, whereas the most intense diffraction peaks of Li_2CN_2 and MgO dominate the XRPD patterns (see Fig. 7a and b). Besides, the characteristic peaks of $Li_4(NH_2)_3BH_4$ are not detected. Simultaneously, some diffraction peaks associated with $Mg(NH_2)_2$ and $Li_2Mg_2(NH)_3$ were identified suggesting that this phase could be an intermediate product of the reaction with CO. FTIR studies (Fig. 8a and b) confirm the presence of Li_2CN_2 (2149 cm^{-1}), $Mg(NH_2)_2$ (3274 cm^{-1}) and $Li_2Mg_2(NH)_3$ (3194 and 3160 cm^{-1}). The bands of $LiNH_2$ were detected but with a slight shift in their positions (3313 and 3258 cm^{-1}), probably due to some kind of disorder in the N–H bond [24]. Extra bands in the region 3650-3200 cm^{-1} correspond to –OH and $-NH_2$ or =NH groups. Moreover, the formation of LiCN (2109 cm^{-1}) was confirmed by FTIR. In the case of the $LiNH_2$-LiH system, the reaction with CO leads to the formation of Li_2O, LiCN and C_3N_4. In addition, pristine $LiNH_2$ and LiH remain after reaction as main phases (Fig. 7). FTIR

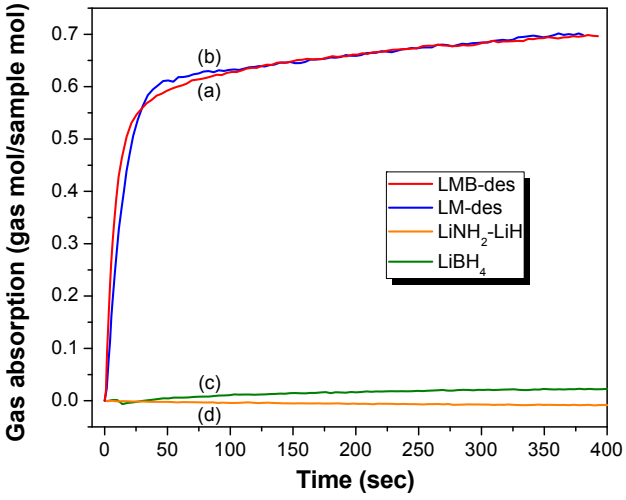

Fig. 6 – Gas consumed (gas mol/sample mol) as a function of time at 200 °C. (a) Dehydrogenated state of LMB composite; (b) Dehydrogenated state of LM composite, both under 1.0 MPa of CO. (c) $LiNH_2$-LiH and (d) $LiBH_4$ under 0.27 MPa of CO.

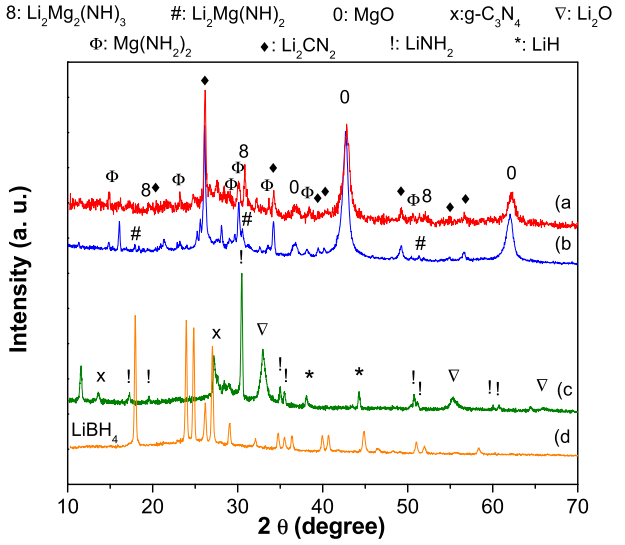

Fig. 7 – XRPD patterns obtained after CO absorption of: (a) Dehydrogenated state of LMB composite; (b) Dehydrogenated state of LM composite, both under 1.0 MPa of CO. (c)$LiNH_2$-LiH and (d) $LiBH_4$ under 0.27 MPa of CO.

confirms the presence of these phases (Fig. 8c). Besides, the characteristic band of Li_2CN_2 was also detected indicating its formation. On the contrary, no new phases were detected after reaction of $LiBH_4$ with CO.

Considering the results displayed in Figs. 7 and 8, the reaction of pure CO with dehydrogenated LM and LMB composites produces MgO and Li_2CN_2 as main final products (Fig. 7) by breaking of the CO bond. The reaction can be represented as:

$$Li_2Mg(NH)_2 + CO \rightarrow Li_2CN_2 + MgO + H_2 \quad (6)$$

The hydrogen produced by reaction (6) is able to react with $Li_2Mg(NH)_2$ as follows:

$$2Li_2Mg(NH)_2 + H_2 \rightarrow Li_2Mg_2(NH)_3 + LiNH_2 + LiH \rightarrow Mg(NH_2)_2 + LiH \quad (7)$$

The hydrogenation of $Li_2Mg(NH)_2$ (reaction 7) promotes reaction (6) according to Le Chatelier's principle. Reactions (6) and (7) are consecutive and the complete process involves a reduction in the gas pressure, in agreement with the behavior observed in Fig. 6 (curves a and b). In fact, the consumption of $Li_2Mg(NH)_2$ was practically complete. The detection of LiCN by FTIR could be due to Li_2CN_2 decomposition. Summarizing, the experimental evidence indicates that the $[NH]^{2-}$ anion reacts faster and stronger with CO (about 0.6 gas mol/sample mol) with respect to $[NH_2]^-$ anion (<0.03 gas mol/sample mol) (Fig. 6). In contrast, $[BH_4]^-$ does not evidence interaction. Then, the decreasing reactivity order with CO is $[NH]^{2-} > [NH_2]^- > [BH_4]^-$.

Regarding the $Li_4(NH_2)_3BH_4$ additive, high CO contents are necessary to favor its reaction in front of $Li_2Mg(NH)_2$ due to different kinetics, as it was mentioned previously. In fact, a broad band at 2100-2300 cm^{-1} due to B-H bond remains. The disappearance of $Li_4(NH_2)_3BH_4$ as a consequence of its reaction with CO affects the mechanism proposed previously for the hydrogen storage reversibility of the LMB composite [19]. In fact, the progressive transformation and/or disappearance of $Li_4(NH_2)_3BH_4$ has to affect the plateau slope of PCI curves.

In the second type of experiment, the LMB composite in the hydrogenated or dehydrogenated states was contacted with a mixture of CO-H_2 (1:8 partial pressure ratio). Hydrogen pressure was selected to ensure the hydrogenated state in the LMB

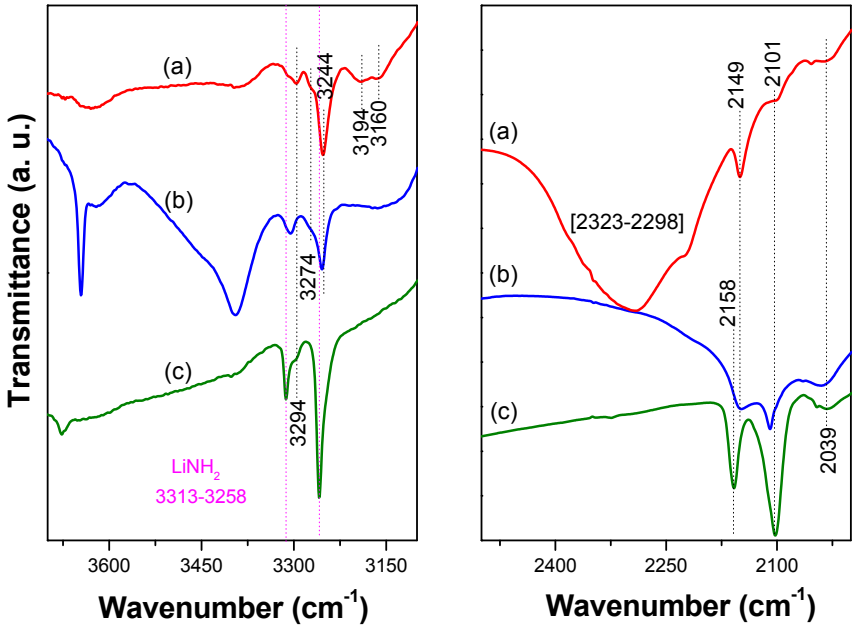

Fig. 8 – FTIR spectra of (a) Dehydrogenated state of LMB composite; (b) Dehydrogenated state of LM composite, both under 1.0 MPa of CO. (c) $LiNH_2$-LiH under 0.27 MPa of CO.

composite (Fig. 9A, curve a) and/or to evidence the competition between CO and H_2 when reacting with the dehydrogenated state (Fig. 9A, curve b). For comparison, the reaction between the dehydrogenated LMB composite with pure CO (0.27 MPa) using the same partial pressure than in the mixture of CO-H_2 was evaluated (Fig. 9, curve c). The amount of gas consumed (gas mol/sample mol) as a function of time at 200 °C is shown in Fig. 9. The fraction absorbed is about 0.1 and 1.4 in 4000 s for the hydrogenated and dehydrogenated LMB composite, respectively (Fig. 9A, curves a and b). In comparison, the curve obtained with pure CO (0.27 MPa) absorbed approximately 0.9 gas mol/sample mol in only 800 s. These results stand out different behavior of the composite depending if it is hydrogenated or dehydrogenated and if CO is diluted in H_2 or pure. In fact, the reaction of the hydrogenated state with CO-H_2 mixture is practically negligible compared to that of the dehydrogenated state. In this last case, $Li_2Mg(NH)_2$ can react with H_2 and CO via rehydrogenation and poisoning, respectively.

XRPD studies performed on the solid products of the reaction with CO-H_2 (Fig. 9B) confirm the nature of the interaction. For the hydrogenated state, the starting phases, *i.e.* $Mg(NH_2)_2$, LiH and $Li_4(NH_2)_3BH_4$ were identified after the reaction with CO. In contrast, the reaction of pure CO (0.27 MPa) with the dehydrogenated state conduced to the formation of MgO and Li_2CN_2 (Fig. 9B, curve c) as well as intermediate phases such as $Mg(NH_2)_2$ and C_3N_4. However, when the CO-H_2 mixture with the same pressure than pure CO is contacted with the dehydrogenated state, hydrogen reacts with the imide phase producing $Mg(NH_2)_2$ and MgO as main final phases. Then, pure CO reacts preferentially with $Li_2Mg(NH)_2$ producing MgO and Li_2CN_2, according to reaction (6). However, the dilution of CO with hydrogen restricts its interaction with the composite by competition with H_2. No reaction of pure CO with $Mg(NH_2)_2$ was detected.

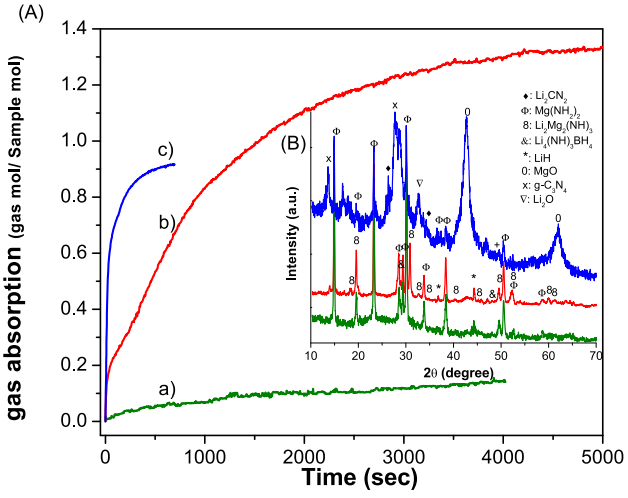

Fig. 9 – (A) Gas absorption (gas mol/sample mol) as a function of time (B) XRPD patterns of the materials obtained after reaction: (a) hydrogenated LMB composite with CO-H_2 mixture (5:40 ratio), (b) Dehydrogenated LMB composite with CO-H_2 mixture (4:32 ratio) and (c) Dehydrogenated state of LMB composite with 0.27 MPa CO.

Conclusions

The hydrogen storage properties of the $Li_4(NH_2)_3BH_4$ doped $Mg(NH_2)_2$-2LiH composite after cycling were evaluated in the presence of CO as impurity. The composite was found to have limited tolerance towards hydrogen cycling with CO (0.1 mol %–H_2 mixture). Although the dehydrogenation kinetics is fast, the hydrogen storage capacity is progressively reduced in 22% after 20 cycles due to irreversible poisoning. The formation of Li_2CN_2 and MgO was confirmed by combination of XRPD and FTIR and it explains the permanent loss of capacity. Specific designed experiments reveal that pure CO easily reacts with $Li_2Mg(NH)_2$ at 200 °C in less than 3 min forming Li_2CN_2 and MgO. Other phases such as $Mg(NH_2)_2$, LiCN and C_3N_4 were detected depending of the CO content, evidencing the complexity of the interaction. No appreciable reaction was detected with the $Mg(NH_2)_2$-2LiH composite. The additive $Li_4(NH_2)_3BH_4$ disappears due to its interaction with high concentrations of CO, remaining the B-H bond intact. In accordance, the reactivity test of the $LiNH_2$-LiH composite against pure CO shows its reaction with the $[NH_2]^-$ group and Li^+, forming Li_2CN_2 and Li_2O, respectively. The CO interaction with $LiBH_4$ was undetected by FTIR and XRPD.

Acknowledgements

This study has been partially supported by CONICET (National Council of Scientific and Technological Research), CNEA (National Commission of Atomic Energy), ANPCyT (Nº 1052) and Instituto Balseiro (University of Cuyo).

REFERENCES

[1] Modibane KD, Williams M, Lototskyy M, Davids MW, Ye Klochko, Pollet BG. Poisoning-tolerant metal hydride materials and their application for hydrogen separation from CO_2/CO containing gas mixtures. Int J Hydrogen Energy 2013;38:9800–10.

[2] Botao Z, Lifei L, Yiming Y, Shilin H, Dong W, Pingzhu Z. Enhanced hydrogen capacity and absorption rate of $LaNi_{4.25}Al_{0.75}$ alloy in impure hydrogen by a combined approach of fluorination and palladium deposition. Int J Hydrogen Energy 2016;41:3465–9.

[3] Dehouche Z, Goyette J, Bose TK, Huot J, Schulz R. Sensitivity of nanocrystalline MgH_2-V hydride composite to the carbon monoxide during a long-term cycling. Nano Lett 2001;1:175–8.

[4] Bouarich S, Huot J, Guay D, Schulz R. Reactivity during cycling of nanocrystalline Mg-based hydrogen storage compounds. Int J Hydrogen Energy 2002;27:909–13.

[5] Kim T-H, Jung-Sik C, Ko-Yeon C, Jae-Suk S, Heondo J, Study on the effect of hydrogen purification with metal hydride, WHEC 16/13–16 June 2006 – Lyon France.

[6] Han S, Xinbo Z, Siqi Si, Hideaki T, Nobuhiro K, Naoki T, et al. Experimental and theoretical investigation of the cycle durability against CO and degradation mechanism of the $LaNi_5$ hydrogen storage alloy. J Alloys Compd 2007;446–447:208–11.

[7] Lototskyy MV, Williams M, Yartys VA, Klochko YeV, Linkov VM. Surface-modified advanced hydrogen storage alloys for hydrogen separation and purification. J Alloys Compd 2011;509S:S555–61.
[8] Lototskyy M, Modibane KD, Williams M, Klochko Ye, Linkov V, Pollet BG. Application of surface-modified metal hydrides for hydrogen separation from gas mixtures containing carbon dioxide and monoxide. J Alloys Compd 2013;580:S382–5.
[9] Borzone EM, Blanco MV, Meyer GO, Baruj A. Cycling performance and hydriding kinetics of $LaNi_5$ and $LaNi_{4.73}Sn_{0.27}$ alloys in the presence of CO. Int J Hydrogen Energy 2014;39:10517–24.
[10] Hu YH, Ruckenstein E. Steam-reforming product (H_2/CO_2 mixture) used as a hydrogen source for hydrogen storage in Li_3N. Ind Eng Chem Res 2007;46:5940–2.
[11] Hu YH, Huo Y. Fast and exothermic reaction of CO_2 and Li_3N into C-N-Containing solid materials. J Phys Chem A 2011;115:11678–81.
[12] Hu YH, Ruckenstein E. Hydrogen storage in $LiNH_2/Li_3N$ material for H_2/CO_2 mixture gas as hydrogen source. Ind Eng Chem Res 2008;47:48–50.
[13] Sun F, Yan M-Y, Liu X-P, Ye J-H, Li Z-N, Wang S-M, et al. Effect of N_2, CH_4 and O_2 on hydrogen storage performance of $2LiNH_2$+MgH_2 system. Int Int J Hydrogen Energy 2015;40:6173–9.
[14] Sun F, Yan M-Y, Liu X-P, Ye J-H, Li Z-N, Wang S-M, et al. Effect of CO on hydrogen storage performance of $2LiNH_2$+MgH_2 system, Int. J Hydrogen Energy 2014;39:9288–92.
[15] Sun F, Yan M-Y, Ye J-H, Liu X-P, Jiang L-J. Effect of CO on hydrogen storage performance of KF doped $2LiNH_2 + MgH_2$ material. J Alloys Compd 2014;616:47–50.
[16] Zhang J, Liu Y, Zhang X, Yang Y, Zhang Q, Jin T, et al. Synthesis of CsH and its effect on the hydrogen storage properties of the $Mg(NH_2)_2$-2LiH system, Int. J Hydrogen Energy 2016;41:11264.
[17] Torre F, Valentoni A, Milanese C, Pistidda C, Marini A, Dornheim M, et al. Kinetic improvement on the CaH_2-catalyzed $Mg(NH_2)_2 + 2LiH$ system. J Alloys Compd 2015;645:S284.
[18] Wang H, Cao H, Wu G, He T, Chen P. The improved hydrogen storage performances of the multi-component composite: $2Mg(NH_2)_2$–3LiH–$LiBH_4$. Energies 2015;8:6898.
[19] Amica G, Cova F, ArneodoLarochette P, Gennari FC. Effective participation of $Li_4(NH_2)_3BH_4$ in the dehydrogenationpathway of the $Mg(NH_2)_2$-2LiH composite. Phys Chem Chem Phys 2016;18:17997–8005.
[20] Li B, Liu Y, Gu Jian, Gu Y, Gao M, Pan H. Mechanistic investigations on significantly improved hydrogen storage performance of the $Ca(BH_4)_2$-added $2LiNH_2/MgH_2$system. Int J Hydrogen Energy 2013;38:5030.
[21] Pan H, Shi S, Liu Y, Li B, Yang Y, Gao M. Improved hydrogen storage kinetics of the Li–Mg–N–H system by addition of $Mg(BH_4)_2$. Dalton Trans 2013;42:3802.
[22] Li B, Liu Y, Li C, Gao M, Pan H. *In situ* formation of lithium fast-ion conductors and improved hydrogen desorption properties of the $LiNH_2$–MgH_2 system with the addition of lithium halides. J Mater. Chem A 2014;2:3155.
[23] Liang C, Liu Y, Wei Z, Jiang Y, Wu F, Gao M, et al. Enhanced dehydrogenation/hydrogenation kinetics of the $Mg(NH_2)_2$-2LiH system with NaOH additive. Int J Hydrogen Energy 2011;36:2137–44.
[24] Gamba NS, ArneodoLarochette P, Gennari FC. $Li_4(NH_2)_3Cl$ amide-chloride: a new synthesis route, and hydrogen storage kinetic and thermodynamic properties. RSC Adv 2016;6:15622–9.